An approach to controlling the fluorescence of graphene quantum dots: From surface oxidation to fluorescent mechanism*

Hu Yin(胡 音)[a], He Da-Wei(何大伟)[a]†, Wang Yong-Sheng(王永生)[a], Duan Jia-Hua(段嘉华)[a], Wang Su-Feng(王素凤)[a], Fu Ming(富 鸣)[a], and Wang Wen-Shuo(王闻硕)[a,b]‡

[a] *Key Laboratory of Luminescence and Optical Information, Ministry of Education, Institute of Optoelectronic Technology, Beijing Jiaotong University, Beijing* 100044, *China*

[b] *Institute of Particle Technology, Friedrich-Alexander University Erlangen-Nuremberg, Cauerstrasse 4, D-91058 Erlangen, Germany*

(Received 7 May 2014; revised manuscript received 23 June 2014; published online 10 October 2014)

We report a facile method of synthesizing graphene quantum dots (GQDs) with tunable emission. The as-prepared GQDs each with a uniform lateral dimension of ca. 6 nm have fine solubility and high stability. The photoluminescence mechanism is further investigated based on the surfacestructure and the photoluminescence behaviors. Based on our discussion, the green fluorescence emission can be attributed to the oxygen functional groups, which could possess broad emission bands within the π–π^* gap. This work is helpful to explain the vague fluorescent mechanism of GQDs, and the reported synthetic method is useful to prepare GQDs with controllable fluorescent colors.

Keywords: graphene quantum dots, tunable luminescence

PACS: 81.05.ue, 73.21.Hb, 87.15.mq **DOI:** 10.1088/1674-1056/23/12/128103

1. Introduction

Graphene, a two-dimensional honeycomb lattice composed of sp^2 carbon atoms has attracted much attention because of its superior electronic, thermal, and mechanical properties that are suited to various applications, such as energy-storage media, optoelectronic devices, sensors, etc.[1–8] Theoretical and experimental studies have shown that quantum confinement could appear in graphene with finite size, named as graphene quantum dots (GQDs).[9] GQDs have numerous applications including catalysis,[10,11] photovoltaic devices,[12,13] bio-imaging,[14] light emitting diodes,[15] etc., owing to their stable photo-luminescences, excellent biocompatibilities, and low cytotoxicities. The primary approaches to fabricating the soluble fluorescent GQDs can be classified into top–down and bottom–up processes. However, the latter one can produce only a small quantity of GQDs, which restricts its application.[16–19] Comparatively, the top–down method involving cutting the graphene sheet through controlled oxidation or the reduction process with low-cost and high yield, has drawn more attention in recent years.[10,11,20–24] Up to now, the main challenges of the top–down synthesis method concentrate on the controllability of the surface oxidation and the tunability of the fluorescence, which requires not only an exquisite synthesis strategy but also clarifying the mystery of the photoluminescence mechanism of GQDs.

In order to extend the application of GQDs, efforts have been made to obtain luminescence tunable GQDs with less expensive precursors and milder conditions. Zhu *et al.* have obtained GQDs with controllable surface oxidation through an efficient two-step separated method involving column chromatography, which induces tunable fluorescence.[14] They gave a possible explanation that a higher degree of surface oxidation would result in more surface defects, making the emission red-shift. Hiroyuki Tetsuka *et al.* demonstrated amino-functionalized GQDs with tunability of photoluminescence.[25] The degree of amine functionalization, which controls the photoluminescence color, can be regulated simply by changing the initial concentration of ammonia or the temperature of the amino-hydrothermal treatment. The resonance feature between the delocalized orbital and the molecular orbital in the $-NH_2$ group is assumed to be an origin of the edge-treatment-dominated optical tunability. In the previous work of our group, we systematically investigated a silver octahedron as a multi-frequency optical antenna employing three-dimensional finite difference time domain (3D-FDTD) calculations.[26] The designed antenna is able to couple efficiently with free space light through multiple localized surface plasma resonances. As a result, the fluorescence can be enhanced and modulated through optimizing the distance and relative 3D configuration between the silver octahedron and the GQDs.

However, the synthesis of GQDs usually involves time-consuming and intricate procedures with strong reaction con-

*Project supported by the National Basic Research Program of China (Grant Nos. 2011CB932700 and 2011CB932703), the National Natural Science Foundation of China (Grant Nos. 61335006, 61378073, and 61077044), and the Beijing Natural Science Foundation, China (Grant No. 4132031).

†Corresponding author. E-mail: dwhe@bjtu.edu.cn

‡Corresponding author. E-mail: wenshuo.wang@fau.de

© 2014 Chinese Physical Society and IOP Publishing Ltd

ditions, or induces complex structures, probably owing to the great difficulty in controlling cleaving the graphene sheets into small pieces on a nanometer scale. In this paper, we report a two-step method of synthesizing water soluble GQDs directly from flake graphite under safe and mild conditions, suggesting its potential for the mass production of GQDs. Flake graphite is one of the most readily obtainable and cheapest precursors of GQDs. Moreover, the emissions of GQDs can be adjusted in the range from 450 nm to 500 nm by controlling the surface oxidation, which expands the applications of the GQDs.

2. Experimental section

2.1. Materials

Flake graphite (325 meshes) was purchased from the Aladdin Chemistry Co., Ltd (Shanghai, China). Sodium nitrate ($NaNO_3$) was bought from the Beijing Chemical Works Co., Ltd (Beijing, China). Potassium permanganate ($KMnO_4$) was purchased from the Beijing Chemical Works Co., Ltd (Beijing, China). Sodium carbonate anhydrous ($NaCO_3$) was bought from the Tianjin Fengchuan Chemical Reagent Technologies Co., Ltd (Tianjin, China). Ultrasound was produced by KQ3200DA (150 W) from the Kun Shan Ultrasonic Instruments Co., Ltd (China). Quinine hemi-sulfate monohydrate (98%) was purchased from Alfa Aesar. Dialysis bag (3500D) was purchased from the Beijing Solarbio Science and Technology Co., Ltd (China). A 220-nm polytetrafluoroethylene (PTFE) microporous membrane was bought from Haining Yibo Filtration Equipment Industry (China).

2.2. Preparation

GQDs were prepared from flake graphite (325 meshes) by a modified method developed by Hummers and Offeman.[27] Flake graphite (3.0 g) was added to concentrated sulfuric acid (300 mL) at room temperature under mechanical stirring, then $NaNO_3$ (43.0 g) was added; afterwards, the mixture was cooled down to 0 °C. $KMnO_4$ (3.0 g) was added slowly under vigorous agitation to keep the temperature of the suspension lower than 20 °C. Successively, a 40-°C water bath was applied to the reaction system and stirred for about 40 minutes. The mixture was further treated under mild ultrasound (150 W) for 3 h. After ultrasound, the reagents turned into an ash black paste. The paste was then diluted with deionized water (200 mL) and converted into a bright brown suspension liquid. The pH value of the diluted solution was adjusted to 7 using Na_2CO_3 followed by filtration through a 220-nm polytetrafluoroethylene (PTFE) microporous membrane before the seeds come out of the oversaturated sulphate and a brown filter solution was then separated. Finally, the solution was dialyzed in a dialysis bag (cut off molecular weight 3500D) in deionized water for 3 days. After the purification, a clear solution with a very light brown color could be obtained.

For modulating the properties of GQDs, the ultrasound power in the experimental phase is varied from 60 W to 150 W.

2.3. Characterizations

A Tecnai G2 F30 transmission electron microscope (TEM) was used to investigate the morphologies of the GQDs. Atomic force microscopy (AFM) images were recorded with an SPM-9600 (Japan). The X-ray photoelectron spectroscopy (XPS) measurement was carried out on PHI Quantera (PHI, Japan), and the binding energy is calibrated with C1s = 284.8 eV. Fluorescence spectra were recorded on an LS 55 Fluorescence Spectrometer (PerkinElmer). Ultraviolet-visible (UV-Vis) spectra were obtained on UV765 from Shanghai Precision & Scientific Instrument Co., Ltd (China).

3. Results and discussion

The water soluble GQDs are prepared by an extremely facile two-step synthesis procedure involving the direct ultrasound of flake graphite in its oxidizing condition at room temperature with substantial purification treatment. Figure 1 is a schematic illustration of the preparation processes of the GQDs. During oxidization, oxygen-containing groups form on the edges and are inserted between the planes of the graphite layers, which renders the layered structure of graphite easily destroyed. In the mean time, epoxy groups tend to form a line on the carbon lattice and the cooperative alignment induces the underlying C–C bonds to break. The presence of these linear defects makes the graphite sheets fragile and readily attacked.[28] Once an epoxy chain appears, it is energetically preferable for it to be further oxidized into epoxy pairs that are then converted into more stable carbonyl pairs at room temperature.[29] As a result, when treated with ultrasound under the oxidative condition, the graphite sheets may further break up into smaller pieces. The mixture is then diluted with deionized water and the pH is adjusted to 7, followed by filtration using a PTFE membrane filter and dialysis in deionized water. After the purification, a clear solution of GQDs with a very light brown color could be obtained, exhibiting the fine solubility of the GQDs. The clear solution emits bright blue–green fluorescence when irradiated with ultraviolet. Here, the ultrasound is critical to the formation of the blue–green luminescent GQDs. The reduction product of the oxidation reactant is removed by the PTFE membrane and the filtrate is further purified using a dialysis bag to obtain pure GQDs. The GQD solution remained homogeneous even after three months of storage at room temperature without any perceptible photoluminescence (PL) changes, indicating the commendable solubility and stability of the GQDs.

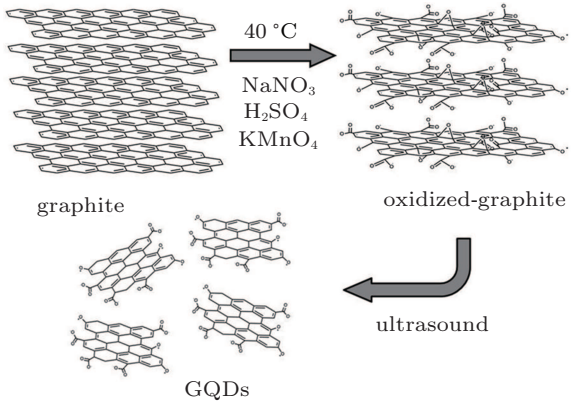


Fig. 1. Schematic illustration of the generation process of GQDs.

Typical morphology characterization results of the resulting GQDs are displayed in Fig. 2. The three batches have similar sizes deduced from TEM characterization. Figure 2 shows the TEM images of GQDs and their size distribution. The average diameters of the GQDs prepared under 60 W, 105 W, and 150 W are 6.20 nm, 6.34 nm, and 5.92 nm, respectively. The diameters of the purified GQDs are mainly distributed in the range of 4 nm–7 nm, indicating that these GQDs have uniform sizes.

Atomic force microscope (AFM) images of the GQDs and the height profiles along the lines are displayed in Figs. 3(a) and 3(b) respectively. The average height of GQDs is 1.44 nm. Consequently, it can be concluded that most of the GQDs are single-layered or double-layered.

The most distinctive feature of the GQDs apart from other reported carbon materials is the specific photoluminescence they emit. Figure 4(a) shows the UV-Vis spectrum of the GQDs aqueous solution. For the GQDs, a typical absorption peak at ca. 230 nm is observed, which is assigned to the π–π^* transition of aromatic sp^2 domains.[2] After that, the curve descends dramatically until ca. 300 nm where it becomes a comparable gentle slope.

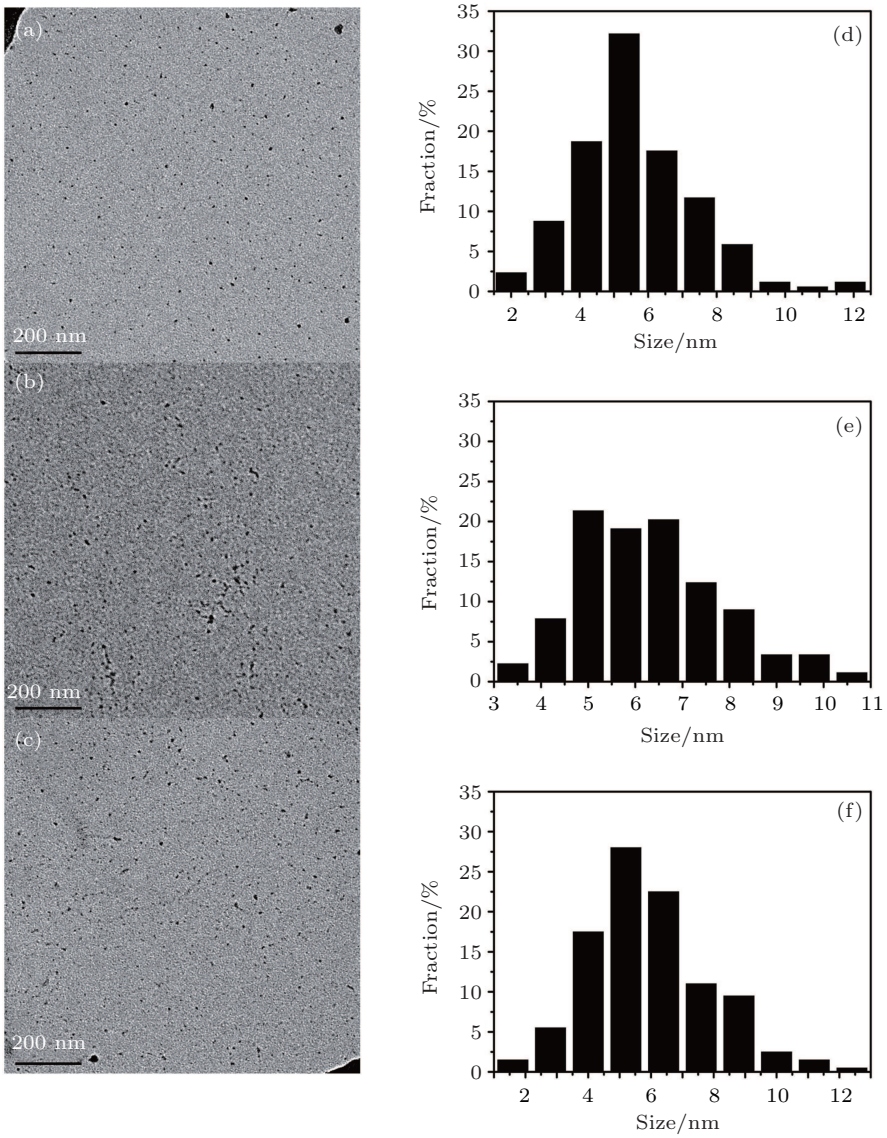


Fig. 2. TEM images of GQDs prepared under ultrasound powers of (a) 60 W, (b) 105 W, and (c) 150 W respectively. Corresponding size distributions of GQDs synthesis under ultrasonication powers of (d) 60 W, (e) 105 W, and (f) 150 W, respectively.

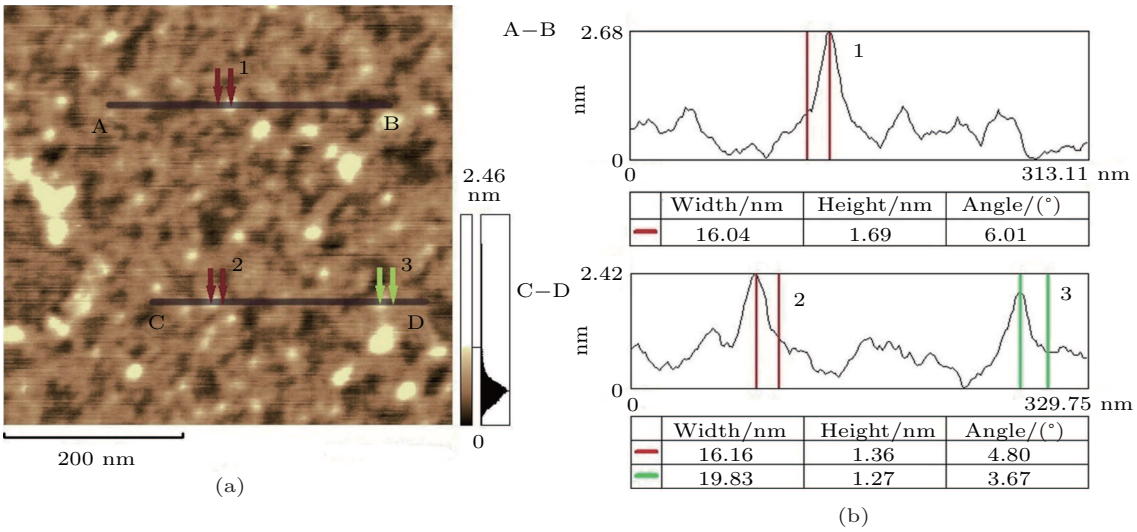


Fig. 3. (color online) (a) AFM image of GQDs and (b) height profiles along the line.

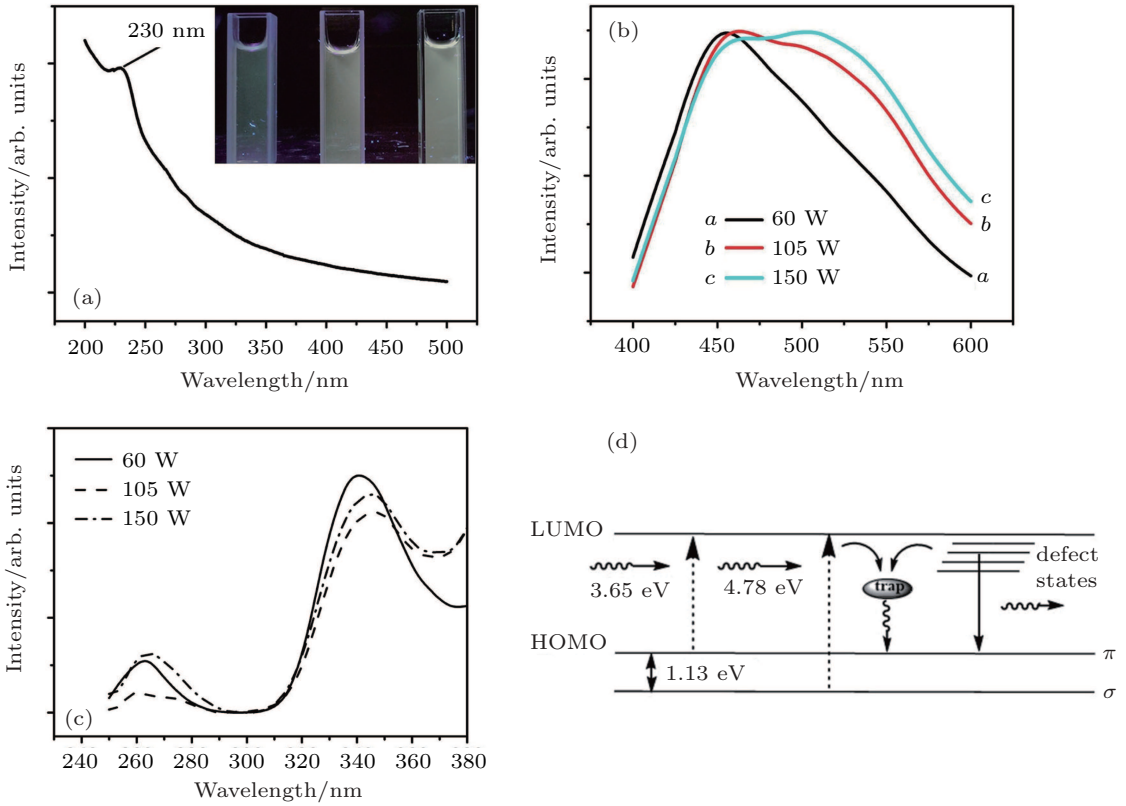


Fig. 4. (color online) (a) UV-visible spectrum of a $GQDs_{60}$ dispersion, with the inset showing the photograph taken under UV light (365 nm). (b) PL spectra of $GQDs_{60}$, $GQDs_{105}$, and $GQDs_{150}$ dispersions recorded at the 340-nm excitation wavelength. (c) PLE spectra of $GQDs_{60}$, $GQDs_{105}$, and $GQDs_{150}$ with the detection wavelengths of 455, 460, and 500 nm, respectively. (d) Schematic illustration of the typical transitions of triple carbenes at zigzag sites.

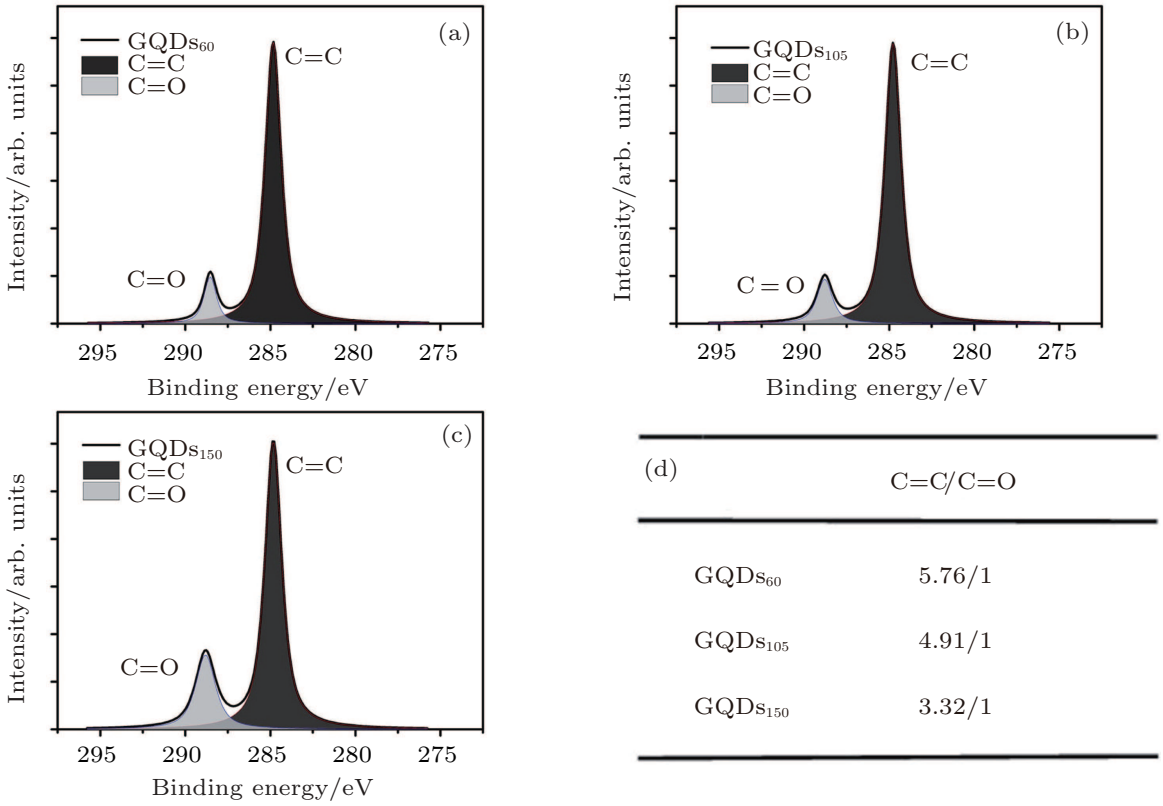
To further explore the optical properties of the water soluble GQDs, an elaborate PL investigation is carried out. As shown in Fig. 4(b), on the excitation wavelength of 340 nm, the GQDs prepared under different ultrasound powers have different fluorescent emission peaks. When the ultrasound power is varied from 60 W to 150 W, the strongest PL peaks of $GQDs_{60}$, $GQDs_{105}$, and $GQDs_{150}$ are 458, 465, and 498 nm, respectively, where the subscripts refer to the ultrasound power as described in Section 2. When treated under an ultrasound power of 60 W, the emission band concentrates at ca. 460 nm where most of the components of the fluorescence are blue. However, when the ultrasound power increases to 105 W, a new band at ca. 500 nm appears where the fluorescence is green. Furthermore, When the ultrasound power rises to 150 W, the blue portion decreases with the enhancement of the green portion. Figure 4(c) shows the photoluminescence

excitation (PLE) spectra of the GQDs prepared at different ultrasound powers. All three kinds of GQDs have PLE peaks at ca. 260 nm and ca. 340 nm, implying that the ultrasound power has little influence on the PLE peaks of GQDs.

All these changes show that the ultrasound treatment exerts a strong influence on the optical properties of the GQDs, but how exactly the fluorescence is affected by the ultrasound condition is to be resolved. The brightness of the PL is quantified in terms of the emission quantum yield using quinine sulfate as the reference according to a literature method.[30] The quantum yields of $GQDs_{60}$, $GQDs_{105}$, and $GQDs_{150}$ obtained at their highest yields are calculated to be 0.59%, 0.38%, and 0.31%, respectively, which are comparable to those previously reported results.[31,32] The quantum yield of GQDs decreases as the ultrasound power is enhanced, probably owing to the non-radiative recombination of localized electron–hole pairs at the non-emissive traps, which suppresses the photoluminescence.[33]

Efforts are made to further explore the origin of the strong luminescence of the GQDs. Despite the fact that the size and the number of layers are noticeably different from particle to particle, all the GQDs studied possess almost the same spectral line-shapes and peak positions, suggesting that they share the same fluorescent origin. Generally, the periphery of micrometer-sized graphene sheets consists of zigzag and armchair edges and free edges that coexist with functionalized edges.[34,35] It is proposed that the luminescence of GQDs should originate from free zigzag sites with a carbene-like triplet ground state. The carbene centers at zigzag sites are stabilized by the localization of itinerant π electrons through σ–π coupling.[34] The two electronic transitions of 260 nm (4.78 eV) and 340 nm (3.65 eV) observed in the PLE spectra can be regarded as being due to the transitions from the σ and π orbits (highest occupied molecular orbits, HOMOs) to the lowest unoccupied molecular orbit (LUMO). Because the two transitions are correlated with the observed PL, the blue–green emission is the irradiation decay of activated electrons from the LUMO to the HOMO as demonstrated in Fig. 4(d). The 260 nm (4.78 eV) and 340 nm (3.65 eV) peaks in PLE spectra can be regraded as being due to the transitions from σ to LUMO and from π to LUMO respectively. The emissions in the PL spectrum can be regared as the decay from defect states (LUMO) to π, with the non-radiative recombination appearing, which might originate from imperfect surface/edge traps. The recombination cannot occur between the defect states and σ bands because no emission with this scale of energy (4.78 eV) has been found in our experiment. The δE is 1.13 eV, which is below 1.5 eV determined by Hoffmann, suggesting that the two transitions are reasonable.[36,37] Previous reports confirmed that defect state emission (surface energy traps) and intrinsic state emission (electron–hole recombination, quantum size effect/zigzag sites) contribute to fluorescence synchronously.[22,38,39] In our experiment, the luminescent of GQDs has two peaks, one is around 453 nm–464 nm (blue emission) and the other is at 504 nm (green emission). The blue emission is attributed to the electron–hole recombination or quantum size effect/zigzag effect (intrinsic state emission), while the green emission is ascribed to being caused by the surface defects (defect state emission).[14] The blue–green luminescence of GQDs is the consequence of the competition between intrinsic state emission and defect state emission. As displayed in the PL image, the blue emission is slightly influenced by the experimental condition, compared with the green emission, which is strongly affected by the ultrasound power, suggesting that the variation of ultrasound power predominantly acts on the defect sate emission rather than intrinsic state emission. With a low oxidation level, the intrinsic state emission plays a leading role in PL behaviors. As the oxidation degree increases, the defect state emission is greatly enhanced, emerging as a competitor against the intrinsic state emission.

Figure 5 shows the X-ray photoelectron spectroscopy (XPS) spectra of the GQDs used to qualitatively and quantitatively characterize the oxygen-containing groups of the GQDs. It can be qualitatively discerned that all kinds of GQDs contain two main peaks at 284.9 eV and 288.8 eV related to C=C and C=O groups respectively. Interestingly, there are no peaks detected at 285.7 eV nor at 286.9 eV, which correspond to the C–OH and C–O–C respectively, compared with previously reported results in Ref. [31]. The spectral results described above reflect that GQDs have oxygenated functional groups on their surfaces, making them soluble in water. Figure 5(d) shows the quantitative calculation results of the relative content between C=C and C=O groups in each GQD sample according to the X-ray photoelectron spectroscopy (XPS) spectrum. The relative amounts of the C=O group content of $GQDs_{60}$, $GQDs_{105}$, $GQDs_{150}$ are 5.2%, 6.0%, and 11.4%, respectively. Apparently, the relative amount of the C=O group content increases with the enhancement of the ultrasound power. Combining the results of the PL spectrum and XPS analysis, we propose that in the ultrasound process, the different ultrasound powers should bring different surface defects into GQDs. It can follow from the XPS and PL results that the stronger power results in more surface defects and correspondingly enhances the defect state emission, which can be used to explain the red-shift phenomenon in our PL spectrum. As a result, the GQDs will have tunable fluorescent emission from blue to green. As for the absence of the C–O–C and C–OH groups, we suppose that in the ultrasound process, the epoxy lines on the planes and the hydroxyl groups on the edges of graphene sheets should further transfer into carboxyl groups.[29]



(d)

	C=C/C=O
$GQDs_{60}$	5.76/1
$GQDs_{105}$	4.91/1
$GQDs_{150}$	3.32/1

Fig. 5. C1s X-ray photoelectron spectroscopy spectra of $GQDs_{60}$ (a), $GQDs_{105}$ (b), and $GQDs_{150}$ (c), where the black and grey areas represent the peak split results of C=C and C=O peaks using XPSPEAK. (d) Quantitative calculation results of the relative content between C=C and C=O groups in each GQD sample according to panels (a), (b), (c).

4. Conclusions

In this study, we successfully prepare water-soluble, uniform sized GQDs with tunable emission through a facile method under moderate conditions. The reported method promotes the synthesis of GQDs as well as the comprehension of the PL mechanism. It is evident that under the given reaction conditions, the oxygen-containing groups form on the GQDs edges in the ultrasound process.

Furthermore, we believe that the oxidation degree on the GQDs is correlated with the ultrasound power, which is verified by control experiments. As the oxidation degree increases with ultrasound power increasing, the emission of the GQDs exhibits red-shift behavior. Finally, the modulation of the photoluminescence is realized only by controlling the oxidation degree of GQDs, which changes the relative proportion between intrinsic emission and defect emission.

References

[1] Geim A K and Novoselov K S 2007 *Nat. Mater.* **6** 183
[2] Novoselov K S, Geim A K, Morozov S V, Jiang D, Zhang Y, Dubonos S V, Grigorieva I V and Firsov A A 2004 *Science* **306** 666
[3] Li D, Mueller M B, Gilje S, Kaner R B and Wallace G G 2008 *Nat. Nanotech.* **3** 101
[4] Choucair M, Thordarson P and Stride J A 2009 *Nat. Nanotech.* **4** 30
[5] Nair R, Blake P, Grigorenko A, Novoselov K, Booth T, Stauber T, Peres N and A Geim 2008 *Science* **320** 1308
[6] Muszynski R, Seger B and Kamat P V 2008 *J. Phys. Chem. C* **112** 5263
[7] Schedin F, Geim A K, Morozov S V, Hill E W, Blake P, Katsnelson M I and Novoselov K S 2007 *Nat. Mater.* **6** 652
[8] Wu H Q, Linghu C Y and Lü H M 2013 *Chin. Phys. B* **22** 098106
[9] Ponomarenko L, Schedin F, Katsnelson M, Yang R, Hill E, Novoselov K and Geim A 2008 *Science* **320** 356
[10] Zhuo S, Shao M and Lee S T 2012 *ACS Nano* **6** 1059
[11] Li Y, Zhao Y, Cheng H, Hu Y, Shi G, Dai L and Qu L 2012 *J. Am. Chem. Soc.* **134** 15
[12] Li Y, Hu Y, Zhao Y, Shi G Q, Deng L E, Hou Y B and Qu L T 2011 *Adv. Mater.* **23** 776
[13] Gupta V, Chaudhary N, Srivastava R, Sharma G D, Bhardwaj R and Chand S 2011 *J. Am. Chem. Soc.* **133** 9960
[14] Zhu S, Zhang J, Tang S, Qiao C, Wang L, Wang H, Liu X, Li B, Li Y and Yu W 2012 *Adv. Funct. Mater.* **22** 4732
[15] Luk C, Tang L, Zhang W, Yu S, Teng K and Lau S 2012 *J. Mater. Chem.* **22** 22378
[16] Liu R, Wu D, Feng X and Müllen K 2011 *J. Am. Chem. Soc.* **133** 15221
[17] Dong Y, Shao J, Chen C, Li H, Wang R, Chi Y, Lin X and Chen G 2012 *Carbon* **50** 4738
[18] Yan X, Cui X and Li L S 2010 *J. Am. Chem. Soc.* **132** 5944
[19] Lu J, Yeo P S E, Gan C K, Wu P and Loh K P 2011 *Nat. Nanotech.* **6** 247
[20] Peng J, Gao W, Gupta B K, Liu Z, Romero-Aburto R, Ge L, Song L, Alemany L B, Zhan X, Gao G, Vithayathil S A, Kaipparettu B A, Marti A A, Hayashi T, Zhu J J and Ajayan P M 2012 *Nano Lett.* **12** 844
[21] Pan D, Guo L, Zhang J, Xi C, Xue Q, Huang H, Li J, Zhang Z, Yu W and Chen Z 2012 *J. Mater. Chem.* **22** 3314
[22] Pan D, Zhang J, Li Z and Wu M 2010 *Adv. Mater.* **22** 734
[23] Yang Z, Li Z H, Xu M H, Ma Y J, Zhang J, Su Y J, Gao F, Wei H and Zhang L Y 2013 *Nano-Micro. Lett.* **5** 247
[24] Xie M M, Su Y J, Lu X N, Zhang Y Z, Yang Z and Zhang Y F 2013 *Mater. Lett.* **93** 161

[25] Tetsuka H, Asahi R, Nagoya A, Okamoto K, Tajima I, Ohta R and Okamoto A 2012 *Adv. Mater.* **24** 5333
[26] Wang W, He D, Duan J, Fu M, Zhang X, Wu H, Hu Y and Wang Y 2014 *Phys. Chem. Chem. Phys.* **16** 4504
[27] Hummers W S Jr and Offeman R E 1958 *J. Am. Chem. Soc.* **80** 1339
[28] Li J L, Kudin K N, McAllister M J, Prud'homme R K, Aksay I A and Car R 2006 *Phys. Rev. Lett.* **96** 176101
[29] Li Z, Zhang W, Luo Y, Yang J and Hou J G 2009 *J. Am. Chem. Soc.* **131** 6320
[30] Sahu S, Behera B, Maiti T K and Mohapatra S 2012 *Chem. Commun.* **48** 8835
[31] Sun Y, Wang S, Li C, Luo P, Tao L, Wei Y and Shi G 2013 *Phys. Chem. Chem. Phys.* **15** 9907
[32] Zhu S, Zhang J, Liu X, Li B, Wang X, Tang S, Meng Q, Li Y, Shi C, Hu R and Yang B 2012 *RSC Adv.* **2** 2717
[33] Mei Q, Zhang K, Guan G, Liu B, Wang S and Zhang Z 2010 *Chem. Commun.* **46** 7319
[34] Radovic L R and Bockrath B 2005 *J. Am. Chem. Soc.* **127** 5917
[35] Li J S, Li Z B and Yao D X 2012 *Chin. Phys. B* **21** 017302
[36] Bourissou D, Guerret O, Gabbai F P and Bertrand G 2000 *Chem. Rev.* **100** 39
[37] Hoffmann R 1968 *J. Am. Chem. Soc.* **90** 1475
[38] Bao L, Zhang Z L, Tian Z Q, Zhang L, Liu C, Lin Y, Qi B and Pang D W 2011 *Adv. Mater.* **23** 5801
[39] Zhu S, Zhang J, Qiao C, Tang S, Li Y, Yuan W, Li B, Tian L, Liu F and Hu R 2011 *Chem. Commun.* **47** 6858